Accepted Manuscript

Role of nanoparticle size, shape and surface chemistry in oral drug delivery

Amrita Banerjee, Jianping Qi, Rohan Gogoi, Jessica Wong, Samir Mitragotri

Please cite this article as: Amrita Banerjee, Jianping Qi, Rohan Gogoi, Jessica Wong, Samir Mitragotri, Role of nanoparticle size, shape and surface chemistry in oral drug delivery, *Journal of Controlled Release* (2016), doi: 10.1016/j.jconrel.2016.07.051

Role of Nanoparticle Size, Shape and Surface Chemistry in Oral Drug Delivery

Amrita Banerjee[1*], Jianping Qi[1, 2*], Rohan Gogoi[3], Jessica Wong[1] and Samir Mitragotri[1,4#]

[1]Department of Chemical Engineering, University of California, Santa Barbara, Santa Barbara, CA 93106, USA, [2]School of Pharmacy, Fudan University, Shanghai 201203, PR China, [3]College of Letters and Science, University of California, Santa Barbara, Santa Barbara, CA 93106, USA, [4]Center for Bioengineering, University of California, Santa Barbara, Santa Barbara, CA 93106, USA

#Address for correspondence:

Prof. Samir Mitragotri

Department of Chemical Engineering, Engineering II, Room 3349,

University of California, Santa Barbara, CA 93106-5080, USA

Phone: (805) 893- 7532

Fax: (805) 893-4731

Email: samir@engineering.ucsb.edu

* These authors have contributed equally.

Abstract

Nanoparticles find intriguing applications in oral drug delivery since they present a large surface area for interactions with the gastrointestinal tract and can be modified in various ways to address the barriers associated with oral delivery. The size, shape and surface chemistry of nanoparticles can greatly impact cellular uptake and efficacy of the treatment. However, the interplay between particle size, shape and surface chemistry has not been well investigated especially for oral drug delivery. To this end, we prepared sphere-, rod- and disc-shaped nanoparticles and conjugated them with targeting ligands to study the influence of size, shape and surface chemistry on their uptake and transport across intestinal cells. A triple co-culture model of intestinal cells was utilized to more closely mimic the intestinal epithelium. Results demonstrated higher cellular uptake of rod-shaped nanoparticles in the co-culture compared to spheres regardless of the presence of active targeting moieties. Transport of nanorods across the intestinal co-culture was also significantly higher than spheres. The findings indicate that nanoparticle-mediated oral drug delivery can be potentially improved with departure from spherical shape which has been traditionally utilized for the design of nanoparticles. We believe that understanding the role of nanoparticle geometry in intestinal uptake and transport will bring forth a paradigm shift in nanoparticle engineering for oral delivery and non-spherical nanoparticles should be further investigated and considered for oral delivery of therapeutic drugs and diagnostic materials.

Keywords: Nanoparticle, Oral delivery, Triple co-culture, Shape, Size, Surface chemistry

Abbreviations

BCA, bicinchoninic acid
CFSE, carborxyfluorescein diacetate succinimidyl ester
DAPI (4',6-diamidino-2-phenylindole, dihydrochloride)
DMEM, Dulbecco's Modified Eagle's Medium
DPBS, Dulbecco's phosphate-buffered saline
EDC, N-(3-dimethylaminopropyl)-N'-ethylcarbodiimide hydrochloride
EDTA, ethylene diamine tetra acetic acid
FBS, fetal bovine serum
HBSS, Hank's balanced salt solution
GIT, gastrointestinal tract
Papp, apparent permeability
PBS, phosphate buffered saline
PEG, polyethylene glycol
PLGA, poly(lactic-co-glycolic acid)
P/S, penicillin/streptomycin
PVA, polyvinyl alcohol
RIPA, radioimmunoprecipitation assay
RPMI-1640, Roswell Park Memorial Institute-1640
SD, standard deviation
SEM, scanning electron microscopy
TEER, trans-epithelial electrical resistance

Introduction

Oral delivery is a preferred route of drug administration. However, due to many challenges associated with oral administration of therapeutic molecules such as low stability in the gastrointestinal tract (GIT) and poor permeability across the intestinal epithelium, many therapeutic drugs are administered as injections to maximize bioavailability [1, 2] . Injectable formulations, though effective, often exhibit decreased patient compliance due to associated needle-phobia that can lead to poor adherence to the treatment and subsequently leads to disease mismanagement, especially for chronic illnesses [3] . Consequently, tremendous emphasis is being placed on engineering novel and effective oral drug delivery systems that significantly improve oral bioavailability [4, 5] . Amongst various approaches, the stability of formulations in the acidic environment of stomach can be improved by coating them with acid stable-pH sensitive polymers such as Eudragit® (poly methacrylate) polymers [6] . Further, encapsulating drugs in a polymeric matrix such as in ethyl cellulose, alginate gels, and mucoadhesive patches can provide gastrointestinal stability against enzymatic degradation [7-10]. In addition, to improve oral bioavailability of many poorly water-soluble drugs, lipids, surfactants and prodrugs have also been used [11, 12] . Nanoparticles also offer a potential means to enhance oral drug bioavailability [13-15] . It has been reported that nanoparticle geometry can significantly impact the interactions with biological targets, thereby bringing about notable differences in formulation efficacy [16-20] . However, the focus of oral delivery using nanoparticles has been limited mostly to spherical particles, which may not be necessarily ideal for many applications.

Here, we explore the role of nanoparticle geometry in oral drug delivery by using polymeric nanoparticles of different sizes (50 – 1000 nm diameter spheres), shapes (spheres, rods and discs) as well as surface chemistry (biotin-conjugated and unconjugated particles). Biotin receptors are present in enterocytes including Caco-2 cells and have been used for oral delivery of biologics [21-24] . We adjudged the efficiency of oral delivery by determining the extent of particle *uptake into* and *transport across* intestinal cells.

Most intestinal drug uptake and permeability studies *in vitro* are conducted using Caco-2 cells that share functional and structural similarity with enterocytes. However, several inadequacies of Caco-2 cells can limit their use for assessing oral uptake and permeability. These include, but are not limited to, absence of other cells that are normally present in the intestinal epithelia and closely work together to form the intestinal barrier, and differences in the tightness of the tight junctions as well as alteration in the expression of efflux pumps compared to human intestine [25, 26] . To more accurately resemble the intestinal epithelia, we utilized a triple co-culture model of intestinal cells comprising Caco-2 cells, HT-29 cells (similar to mucus producing goblet cells) and Raji-B lymphocytes (induces M cell type phenotype when co-cultured with Caco-2 cells) [26, 27] . All these cells are involved in drug absorption and transportation across the intestine and the model has been recently utilized for studying nanoparticle transport [28] .

The results of the study indicated that rod shaped particles are taken up and transported across the intestinal cells to a greater extent compared to their spherical counterparts. Inclusion of targeting ligand on the particles further enhanced cellular uptake of rod shaped particles. The study points to the fact that it is critical to evaluate the effect of nanoparticle geometry in oral drug delivery prior to their utilization for therapy.

Materials and Methods

Materials

Fluoresbrite® carboxylate polystyrene particles were purchased from Polysciences Inc. (Warrington, PA, USA). Polyvinyl alcohol, bovine serum albumin, N-(3-dimethylaminopropyl)-N'-ethylcarbodiimide hydrochloride (EDC), carboxyfluorescein diacetate succinimidyl ester (CFSE), Alcian blue 8GX and SIGMAFAST[TM] fast red TR/naphthol AS-MX tablets were purchased from Sigma Aldrich (St Louis, MO, USA). EZ-link® amine-polyethylene glycol 2 (PEG2)-biotin, Pierce® (radioimmunoprecipitation assay) RIPA buffer, fluorescence biotin quantitation kit and micro bicinchoninic acid (BCA)® protein assay kits were purchased from Thermo Scientific (Rockford, IL, USA). Paraformaldehyde (16% w/v) was obtained from Alfa Aesar (Ward Hill, MA, USA). Vectashield Hardset[TM] with 4',6-diamidino-2-phenylindole, dihydrochloride (DAPI) was purchased from Vector laboratories Inc. (Burlingame, CA, USA). Millicell®-PCF cell culture inserts (3.0 μm pore size, 12 mm diameter) were purchased from Merck Millipore Ltd (Billerica, MA, USA). Dulbecco's Modified Eagle's Medium (DMEM) of Gibco[TM] with and within phenol red were purchased from Thermo Scientific (Rockford, IL, USA). Roswell Park Memorial Institute-1640 (RPMI 1640), fetal bovine serum (FBS), penicillin-streptomycin solution, 0.25% trypsin solution, Hank's balanced salt solution (HBSS) and Dulbecco's phosphate-buffered saline (DPBS) were obtained from GE Healthcare Bio-Sciences (Marlborough, MA, USA). All other reagents were of analytical grade.

Preparation of different shaped nanoparticles

Polystyrene sphere-, rod- and disc-shaped particles were prepared from polystyrene spherical particles using the film-stretching procedure described in our earlier reports [20, 29] . Briefly, 200 nm sized fluorescent spheres with free carboxyl terminus were suspended in 10% polyvinyl alcohol (PVA) solution containing 2% glycerol as plasticizer. The suspension was poured on a 19 x 27 cm flat station and was allowed to dry to form a film. The films were then stretched in one or two directions by using custom-made stretching apparatus. Stretching was conducted at 120 °C in an oil bath. Particle dimensions were controlled by the amount of stretching imposed on the film based on pre-determined aspect ratios. An aspect ratio of 2 was used for rods (in one direction) and discs (in two directions). Thereafter, the stretched films were allowed to cool to room temperature and cut into small pieces which were dissolved in water at 65 °C. The particles were washed by centrifugation in the same solution to remove PVA from the surface of the particles. To obtain spheres, films were not stretched but directly dissolved in hot water and centrifuged. Utilization of spheres obtained from films ensured that the surface of spheres, rods and discs were similar with respect to any residual PVA

coating on the surface, therefore allowed for proper comparison between the particles for cellular uptake and transport.

Conjugation of nanoparticles with biotin

Carbodiimide crosslinker chemistry was used to conjugate nanoparticles with EZ-link[®] amine-PEG_2-biotin [16] . Briefly, the nanoparticles, including spheres, rods and discs, were centrifuged and re-suspended to 1 mg/mL concentration using citric acid buffer (pH 5.0, 20 mM). EDC was then added to the nanoparticle suspension to activate the free carboxyl terminus and the mixture was vortexed/sonicated for 15 min. Thereafter, the nanoparticles were spun down to remove excess EDC. The particles were then re-suspended in citrate buffer containing 1 mg/ml amine-PEG_2-biotin and kept overnight for conjugation under 4 °C. The nanoparticles obtained the following day were washed three times with PBS to remove any unspecific adsorption of biotin molecules on the particle surface and biotin density on the surface of nanoparticles was measured using a fluorescence biotin quantitation kit.

Characterization of nanoparticles

The particle size and zeta potential of nanoparticles were measured using Zetasizer Nano (Malvern Instruments, Malvern, UK) equipped with a 4 mW He-Ne laser (633nm) at 25 °C. The shape of nanoparticles was evaluated using scanning electron microscope (SEM) FEI Nova Nano 650 FEG SEM (Hillsboro, OR), equipped with Oxford Inca X-ray EDX system detector (Abingdon, Oxfordshire, UK). The particles were sputter coated with gold/palladium alloy before analysis and a beam voltage of 5 kV and 50,000 x magnification was used for imaging.

Cell culture and establishment of cell model

Caco-2 cells were cultured in high glucose DMEM culture media with 10% FBS and 1% P/S at 37 °C, 90% relative humidity and 5% CO_2 in T-175 flasks. The cells were passaged every week using 0.25% trypsin/0.02% EDTA solution when the cell confluence in the flasks reached around 80%. HT-29 cells were cultured by the same procedure as Caco-2 cells. For Raji-B cells, RMPI 1640 culture medium was used instead of DMEM.

For establishment of the cell model, Caco-2 cells were seeded onto the Millicell[®]-PCF inserts placed in 24-well plates at a density of $2x10^5$ cells/ml under regular culturing conditions. The culture medium was changed every other day for the first week, and every-day for the following two weeks. After 14-21 days of culturing, the trans-epithelial electrical resistance (TEER) was measured, and the Caco-2 monolayer with more than 300 $\Omega \cdot cm^2$ of TEER value was used for transmembrane transport studies.

The co-culture models of Caco-2/HT-29 and Caco-2/HT-29/Raji-B were established and validated according to previously reported procedures [30] . Caco-2 and HT-29 were seeded into Millicell[®]-PCF insert together in a population ration of 7:3. The seeding of HT-29 cells was validated by Alcian blue staining. Raji-B cells were

introduced into Caco-2 or Caco-2/HT-29 cells to the basal side at a density of $2x10^6$ cells/ml to model the intestinal M cells. The Caco-2 or Caco-2/HT-29 cells with TEER over 300 $\Omega \cdot cm^2$ were further cultured for 3 days after addition of Raji-B cells. TEER values were monitored each day until significant decrease in TEER to around 150-200 $\Omega \cdot cm^2$ was observed, which indicated the successful infiltration of Raji-B cells into the Caco-2 or Caco-2/HT-29 monolayers. To validate, Raji-B cells were stained green using CFSE and the basal side of the culture film was observed by confocal microscopy to the identify Raji-B cells.

Cellular uptake study

Caco-2 cells were seeded in 24-well plates for quantitation of uptake and into petri dishes for confocal microscopy at a density of $2x10^5$ cells/ml following the regular culturing procedures. The culture medium was changed every other day. For Caco-2/HT-29 co-culture, Caco-2 and HT-29 cells were seeded in a population ratio of 7:3 using the same procedure as Caco-2 cells. After 14 days, the cell model was ready for the uptake study. The culture media were discarded and washed with HBSS three times. Then 400 μl nanoparticle suspension at a concentration of 100 μg/ml in phenol red free DMEM was added into each well. After 5 h incubation, the donor solution was discarded and washed with HBSS three times. Cells were broken using 200 μl Pierce® RIPA buffer. The nanoparticle concentration was then measured by fluorescence and protein content was measured by micro BCA® assay kit.

Transport across cells

For transport studies to evaluate effects of size, shape and surface modification, Caco-2, Caco-2/HT-29, Caco-2/Raji-B and Caco-2/HT-29/Raji-B cells were employed. When the cells were ready, they were washed three times using HBSS. Thereafter, 400 μL nanoparticles (100 μg/mL) in phenol red free medium containing 1% BSA was added to the apical side and 600 μl of the same medium (but without the particles – blank medium) was added to basal side. Samples of 100 μl were withdrawn from the basal side at various time intervals (0.5, 1, 2, 3, 4 and 5 hours) and replaced immediately with 100 μl blank medium. The concentration of nanoparticles in samples was measured directly for fluorescence using a Tecan Infinite M200 Pro multimode reader (Tecan US, Inc, Morrrisville, NC, USA microplate reader). After 5 hours, the apical side was washed with HBSS three times and 100 μl paraformaldehyde (4% w/v) was added to apical side for fixing the cells. The membrane with the cells were then cut out, stained with DAPI and observed under confocal microscope.

Data Analysis

All data are represented as mean ± standard deviation (SD). The graphs were plotted using Graphpad, Prism 6.0, (GraphPad Software, LaJolla, CA). Statistical analyses were conducted using Student's T-Test and a value of $p < 0.05$ was considered statistically significant.

Results

Characterization of nanoparticles

The nanoparticles were characterized based on their size, charge, shape and surface density of conjugated biotin (Tables 1 and 2). The sizes of unmodified spherical nanoparticles (i.e. spherical particles that were not subjected to films) had a size range similar to their respective manufacturer labels (Table 1). They are represented in the table with respect to their diameters (50 – 1000 nm) while particles obtained from films are represented with respect to their shapes (spheres, rods and discs). As evident from the low PDI values, particle size was quite uniform and biotin conjugation did not significantly increase the size. The particles were inherently negative in charge due to the presence of carboxyl terminus residues. Unmodified spheres were highly negatively charged with zeta potential values ranging between -30 to -60 mV, while particles derived from films were slightly less negative compared to original particles, possibly due to presence of residual film material on the surface of particles. Conjugation of biotin to particles greatly reduced their charge. The loss of negative charges in the ligand-conjugated particles suggests successful conjugation of biotin to particles.

Table 1. Size (hydrodynamic diameter) and charge of nanoparticles of various sizes, shapes and surface chemistries

Particles	Size (nm)	PDI	Zeta potential (mV)
50 nm	65.3 ± 0.3	0.111 ± 0.03	-59.8 ± 0.7
200 nm	220.0 ± 4.3	0.034 ± 0.02	-47.4 ± 1.6
500 nm	588.7 ± 17.5	0.497 ± 0.16	-48.6 ± 2.7
1000 nm	961.5 ± 19.2	0.053 ± 0.05	-29.8 ± 0.5
Sphere	245.1 ± 2.1	0.023 ± 0.02	-12.9 ± 0.2
Biotin-Sphere	283.7 ± 1.7	0.08 ± 0.02	-4.4 ± 0.1
Rod	394.1 ± 3.5	0.075 ± 0.07	-11.8 ± 1.1
Biotin-Rod	399.5 ± 1.2	0.192 ± 0.004	-2.2 ± 0.1
Disc	293.1 ± 5.1	0.122 ± 0.02	-13.9 ± 2.6
Biotin-Disc	367.8 ± 14.3	0.275 ± 0.02	-4.1 ± 0.2

Biotin concentration on particle surface was evaluated using biotin quantitation fluorescence kit. The concentration of the molecules on the particles were in the range of 5.7 – 8.4 pmol/µg particles (Table 2).

Table 2: Concentration of biotin molecules on nanoparticles

	Biotin density (pmol/µg nanoparticles)
Biotin-Sphere	7.17 ± 0.64
Biotin-Rod	8.38 ± 0.31
Biotin-Disc	5.67 ± 0.09

The SEM images of both unconjugated and biotin-conjugated spheres, rods and discs revealed particle sizes in accordance with the size obtained from dynamic light scattering. No difference was found in the size of conjugated and unconjugated spheres, rods and

discs. Spheres were seen in the size range of 200 - 220 nm, while rods had a longitudinal dimension of 400 – 500 nm and width approximately between 125 – 175 nm. Discs were in the size range of 300 – 350 nm across both cross dimensions (Fig. 1).
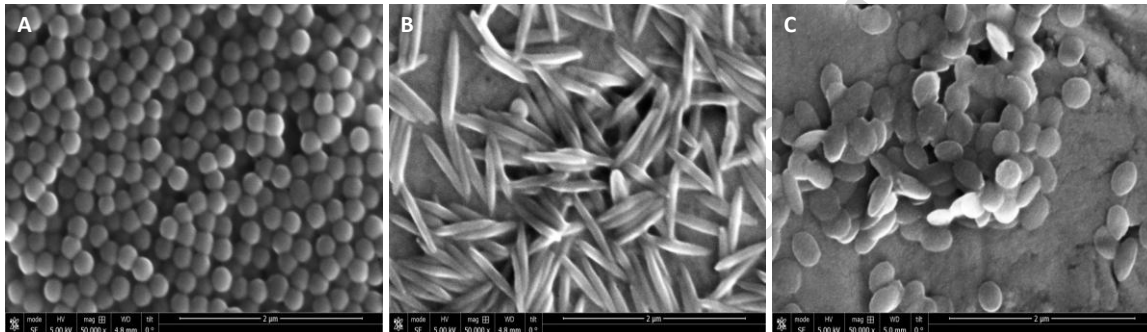

Figure 1: Scanning electron microscopy images of nanoparticles of different shapes. Representative scanning electron microscopy images of A) spheres; B) rods; and C) discs.

Effect of Size on Uptake and Transport of Nanoparticles Across Intestinal Cells

Uptake of Particles

Particle uptake by Caco-2 and Caco-2/HT-29 cells was inversely related to their size, with uptake of 50 nm > 200 nm > 500 nm > 1000 nm (Fig. 2). The uptake of particles of all sizes was consistently higher in Caco-2/HT-29 cells compared to Caco-2 monolayers. Confocal micrographs also clearly depicted the cellular uptake trend of different sized particles by Caco-2/HT-29 cells (Fig. 3).
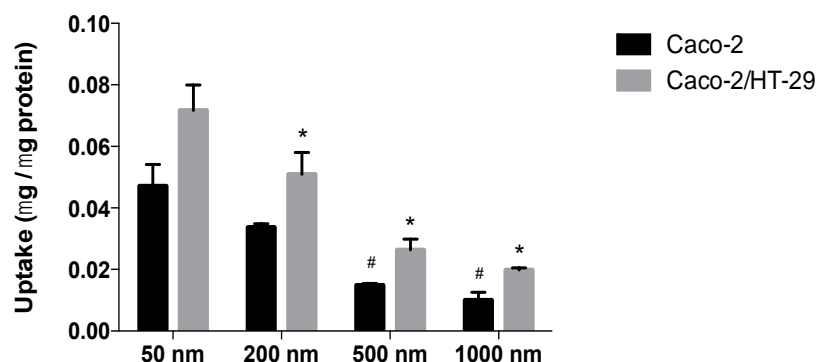

Figure 2: Uptake of different sized nanoparticles by Caco-2 cells (black bars) and Caco-2/HT-29 cells (grey bars). The uptake of 50 and 200 nm spheres was significantly higher than 500 and 1000 nm spheres in Caco-2 cells while in Caco-2/HT-29 cells, the uptake of 50 nm particles were significantly higher than all other sizes. Uptake of 200 nm spheres was significantly higher than 500 nm and 1000 nm spheres. * represents significant difference compared to 50 nm particles in Caco-2/HT-29 cells while # represents significant difference compared to 50 nm particles

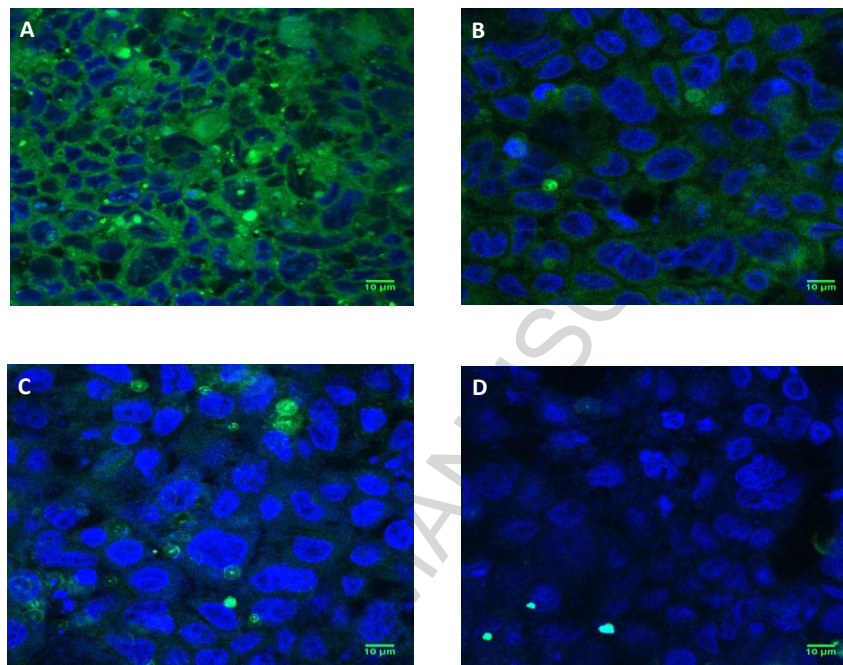**in Caco-2 ($p < 0.05$). Data represented as mean ± SD.**

Figure 3: Confocal micrographs of uptake of different sized nanoparticles by Caco-2/HT-29 cells. Representative confocal microscopy images showing uptake of A) 50 nm spheres; B) 200 nm spheres; C) 500 nm spheres and D) 1000 nm spheres by Caco-2/HT-29 cells at the end of 5 h of study. Green fluorescence represents particles while blue color represents cell nuclei (DAPI staining). Scale bar = 10 μm. Smaller sized particles were taken up to a higher extent compared to larger sized particles.

Transport across Monolayers

To evaluate the effect of size of nanoparticles on their transport across intestinal cells, unmodified spheres of different sizes (50, 200, 500 and 1000 nm) were incubated with Caco-2 monolayer, and co-cultures of Caco-2/Raji-B, Caco-2/HT-29 and Caco-2/HT-29/Raji-B cells. Transport of different sized particles across Caco-2 monolayer was minimal and did not depend on size (Fig. 4A). A maximum transport of about 0.3% was observed after 5 h for 50 nm sized particles. This is in agreement with previous report on transport of non-biodegradable nanoparticles across Caco-2 monolayers where it has been reported that Caco-2 cells can easily take up intact particles but not transport them across the monolayer [30] . On the contrary, transport across Caco-2/Raji-B cells was significantly higher and showed differences between various sized particles (Fig. 4B). The highest transport was observed for 50 nm sized particles to up to 25% in 5 h but it was not significantly different from 200 nm shaped particles where the maximum transport after 5 h was found to be ~22%. On the other hand, transport of 500 and 1000 nm sized particles was significantly lower with a maximal transport of 15% and 8% respectively after 5 h. The transport of particles across Caco-2/HT-29 cells showed

similar transport profile as observed for Caco-2 monolayers (Fig. 4C). No difference was found between the different sized particles and a maximum transport of ~0.4% was observed after 4 h for 50 nm particles. In the triple co-culture, 50 and 200 nm sized particles showed significantly higher
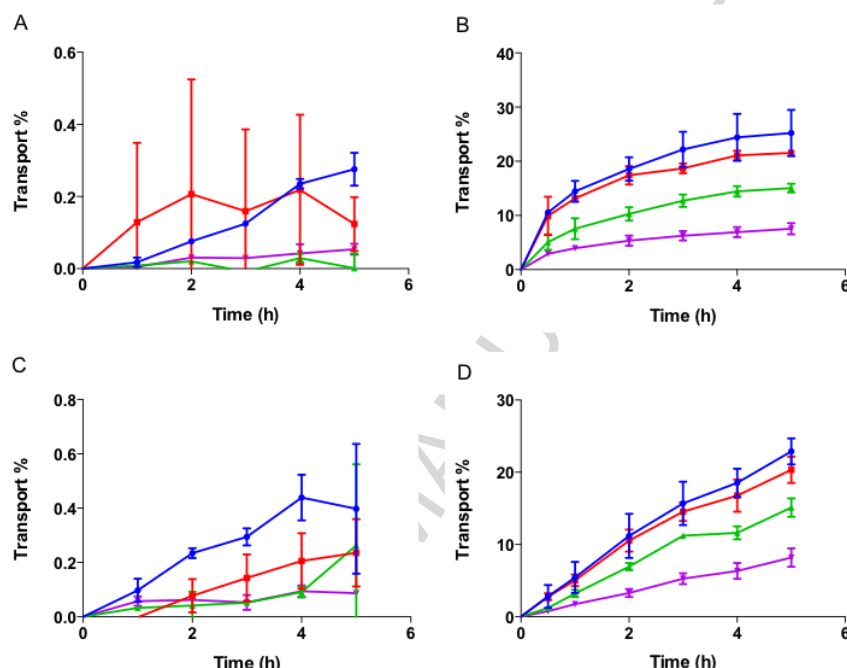

Figure 4: Transport of different sized nanoparticles across intestinal cells. Transport of nanoparticles across (A) Caco-2 cells; (B) Caco-2/Raji-B; (C) Caco-2/HT-29 and (D) Caco-2/HT-29/Raji-B cells. Different particle sizes are represented as blue circles (50 nm), red squares (200 nm), green upright triangles (500 nm) and purple downward triangles (1000 nm). No significant transport of particles across Caco-2 monolayer or Caco-2/HT-29 cells was observed. Inclusion of Raji-B cells into the cell culture, improved transport significantly and demonstrated size dependent effect. Smaller particles (50 and 200 nm) were transported more efficiently than larger particles (500 and 1000 nm) across Raji-B based co-cultures. Data represented as mean ± SD.

transport of more than 20% at the end of 5 h compared to 500 and 1000 nm sized particles where 15% and 8% transport was observed respectively over time (Fig. 4D). Confocal images of transwell membranes seeded with triple co-culture at the end of transport experiments using different sized particles are presented in supplementary Fig S1. The results demonstrate that Raji-B cells are essential for transport of nanoparticles across the transwells, which is in agreement with previous reports where presence of lymphocytes was found to increase transport of nanoparticles across Caco-2 co-cultures significantly [31-33] .

Effect of Shape on Uptake and Transport of Nanoparticles Across Intestinal Cells

Uptake by Cells

The uptake of different shaped nanoparticles by intestinal cells was studied using spheres, rods and discs that were prepared by stretching 200 nm spheres in either one dimension (rods) or in two dimensions (discs). The uptake of rods and discs was significantly higher than spheres in Caco-2 cells but there was no difference between the uptake of rods and discs (Fig. 5). In Caco-2/HT-29 cells however, the uptake of rods was significantly higher than both spheres and discs (Fig 6). Confocal images of uptake of different shaped nanoparticles in Caco-2/HT-29 cells also clearly illustrate that rods are taken up to a greater extent than spheres and discs (Fig 7 A, B and C).
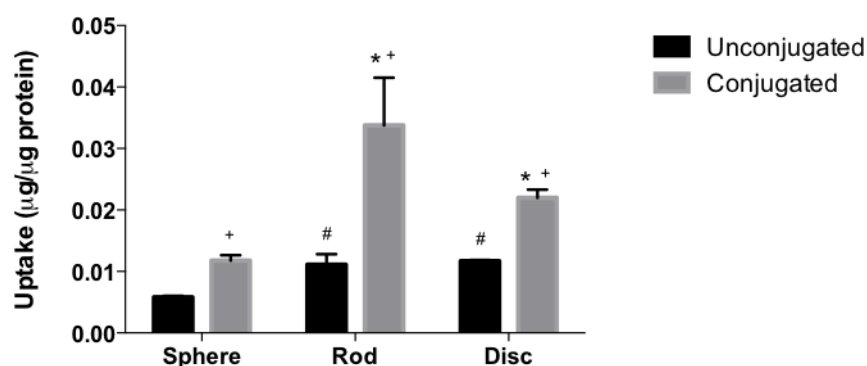

Figure 5: Uptake of biotin conjugated (black bars) and unconjugated nanoparticles (grey bars) by Caco-2 cells. Biotin conjugation significantly improved uptake of particles of all shapes in Caco-2 cells; while biotin conjugated and unconjugated rods and discs demonstrated higher uptake than conjugated and unconjugated spheres respectively. # represents significant difference compared to unconjugated spheres, * represents significant difference compared to conjugated spheres and + represents significant difference between conjugated and unconjugated particles, ($p < 0.05$). Data represented as mean ± SD.
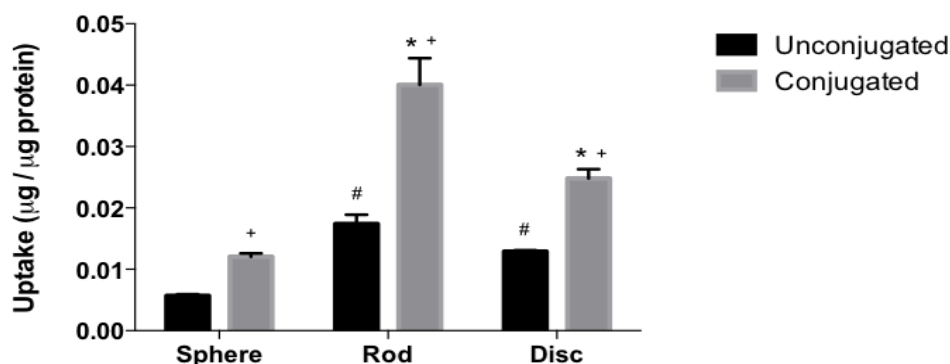
Figure 6: Uptake of unconjugated and biotin conjugated nanoparticles by Caco-2/HT-29 cells. Uptake of unconjugated (grey bars) and biotin conjugated (black bars) nanoparticles by Caco-2/HT-29 cells. Biotin conjugation significantly improved uptake of particles of all shaped particles in Caco-2/HT-29 cells; while biotin conjugated and unconjugated rods and discs demonstrated higher uptake than conjugated and unconjugated spheres respectively. # represents significant difference compared to unconjugated spheres, * represents significant difference compared to conjugated spheres and + represents significant difference between conjugated and unconjugated particles, (p < 0.05). Data represented as mean ± SD.

Transport

The effect of nanoparticle shape on their transport across intestinal cells was also evaluated using spheres, rods and discs. No significant transport of differently shaped particles was seen across Caco-2 monolayers (Fig. 8A). A maximum transport of about 0.5% of total particles was observed at the end of 5 h for all the different shaped particles. In Caco-2/Raji-B co-culture, the transport increased to up to 20% for both rods and discs (Fig. 8B). Spheres were transported to a lesser degree to about 14% by 5 h. On the other hand, particle transport across Caco-2/HT-29 cells did not show any difference between different shaped particles (Fig. 8C). A maximum transport of about 1% was observed for spheres after 5 h that was not significantly different from that observed for rods and discs. The transport profile of particles across the triple co-culture was similar to that of Caco-2/Raji-B co-culture (Fig. 8D). Discs showed the highest transport of about 18% at the end of 5 h but the transport was not significantly different from that of rods (~15%). The transport of spheres was less than that of rods and discs with a maximum transport of about 11% at the end of 5 h. The study clearly indicated that rods and discs are transported to a greater extent across intestinal cells compared to spheres. Confocal images of transwell membranes after the end of transport experiment using triple co-culture are consistent with this observation (suppl. Fig. S2). The fluorescence of particles decreases by 1.5 and 3 fold when stretched into rods and discs respectively compared to spheres, and should be taken into consideration while inspecting the confocal images of different shaped particles. Note that for quantification purposes, the reduced fluorescence of discs and rods was taken into consideration via using corresponding particles for determining calibration curves.
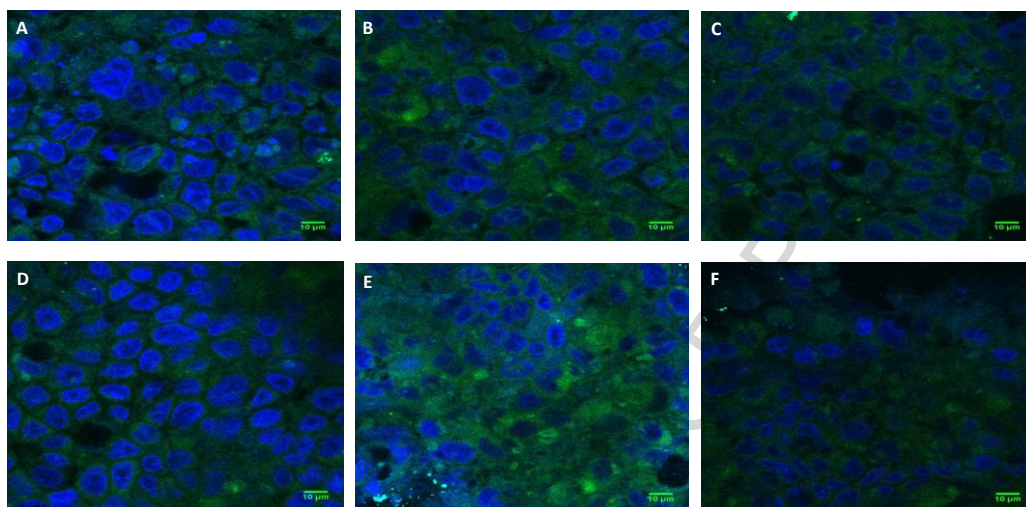
Figure 7: Confocal micrographs of uptake of nanoparticles of different shapes and surface chemistries by Caco-2/HT-29 cells. Representative confocal microscopy images showing uptake of A) Spheres; B) Rods; C) Discs; D) Biotin conjugated Spheres; E) Biotin-conjugated Rods and F) Biotin-conjugated Discs by Caco-2/HT-29 cells at the end of 5 h of study. Green fluorescence represents particles while blue color represents cell nuclei (DAPI staining). Scale bar = 10 μm. It is to be noted that upon stretching 200 nm spheres into rods and discs, the fluorescence of the stretched particles diminishes by approximately 1.5 and 3 fold respectively compared to spheres. Therefore, despite attenuated fluorescence, rods demonstrate higher uptake than spheres in Caco-2/HT-29 cells.

Effect of Surface Modification on Uptake and Transport of Nanoparticles Across Intestinal Cells

Uptake in Cells

The effect of active targeting on intestinal uptake of differently shaped nanoparticles was studied using biotin-conjugated spheres, rods and discs. Conjugated particles of all shapes demonstrated significantly higher uptake in both Caco-2 and Caco-2/HT-29 cells compared to their unconjugated counterparts (Figs. 5 and 6 respectively). In both Caco-2 and Caco-2/HT-29 cells, the uptake of conjugated rods was 3 and 2.5 fold higher respectively compared to unconjugated rods. The uptake of biotin-conjugated rods was also significantly higher than biotin-conjugated spheres and discs in both Caco-2 and Caco-2/HT-29 cells while biotin-conjugated discs demonstrated significantly higher uptake than biotin-conjugated spheres. The study clearly indicated that biotin receptor-mediated targeting considerably improves cellular uptake of rods in both Caco-2 and Caco-2/HT-29 cells compared to non-targeted rods or targeted/non-targeted spheres and discs. Confocal microscopy images also clearly illustrate that rods have higher cellular uptake than spheres and discs in Caco-2/HT-29 cells (Figs. 7 D, E and F).

Transport across Monolayers

Transport of biotin conjugated spheres, rods and discs was studied to evaluate whether surface modification results in significant differences in their transport across intestinal cells. As observed earlier with unconjugated nanoparticles, no significant transport was observed for conjugated spheres, rods or discs across Caco-2 monolayer and Caco-2/HT-29 co-culture (Figs. 9 A and C respectively). No difference in transport between the different shapes was observed in both cell cultures. Consistent with our previous observation, the transport of conjugated particles was higher across Caco-2/Raji-B cells (Fig 9 B). Rods were transported to the highest extent (~27%), followed closely by discs (~23%). On the contrary, spheres were transported to a significantly lower extent to a maximum about 13% by 5 h. In the triple co-culture, 18% and 21% of conjugated rods and discs were transported respectively (Fig. 9 D). Spheres, on the other hand were transported only to about 12% by the end of the study. The percent transport of biotin-conjugated particles was similar to that of unconjugated particles, with the exception of conjugated rods that showed significantly higher transport compared to unconjugated rods across the triple co-culture. This may be attributed to the fact that Caco-2 cells, which display biotin receptors, are not primarily responsible for transcytosis of nanoparticles across the cells [30] . Therefore, surface modification considerably improved uptake but did not increase transport. Confocal microscopy images of transwell membranes taken after the end of transport experiment using triple co-culture show that conjugated rods have higher transport compared to conjugated spheres (suppl. Fig. S3).
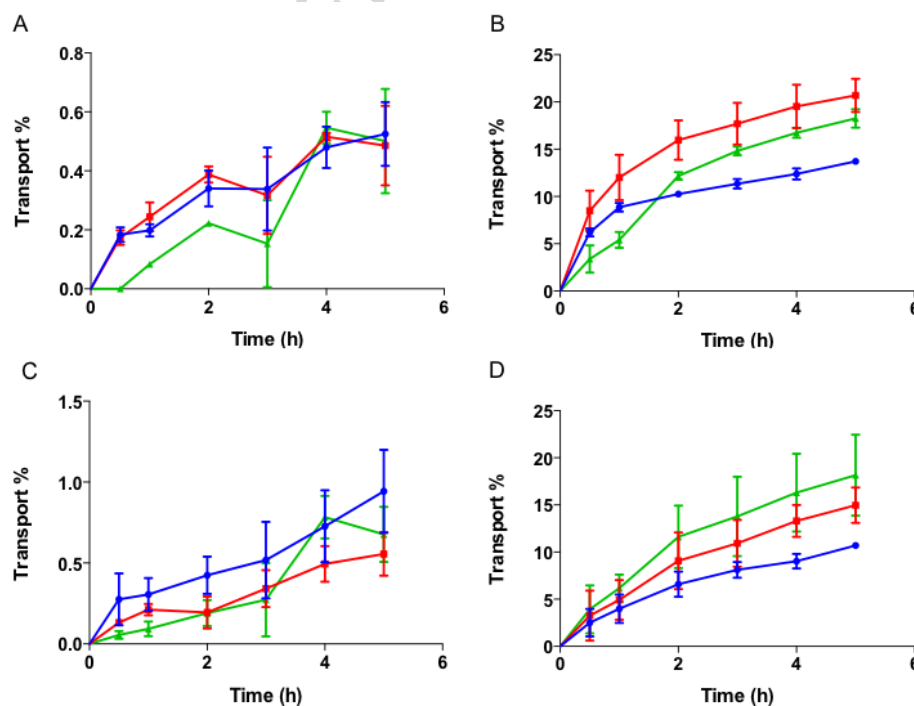

Figure 8: Transport of different shaped nanoparticles across intestinal cells. Transport of spheres, rods and discs across (A) Caco-2; (B) Caco-2/Raji-B; (C) Caco-2/HT-29 and (D) Caco-2/HT-29/Raji-B cells. Spheres, rods and discs are

15

represented as blue circles, red squares and green triangles respectively. No significant transport of particles across Caco-2 monolayer or Caco-2/HT-29 cells was observed. Inclusion of Raji-B cells into the cell culture, improved transport significantly and demonstrated shape dependent effect. Rods and discs were transported more than spheres across Raji-B based co-cultures. Data represented as mean ± SD.

Discussion

Oral drug delivery, owing to its non-invasiveness and high patient compliance, is a highly sought after route for drug administration. In addition, the large surface area for absorption in the intestine along with the presence of M cells in various parts of the intestine provide a high incentive for delivery of therapeutic drugs orally. However, despite the advantages, drug delivery through the oral route faces many challenges. This includes rapid drug degradation in the gastrointestinal tract due to acidic environment in the stomach and proteolytic enzymes present in the intestine as well as physiological barrier for absorption due to the presence of tight junctions in the intestine. Moreover, the physico-chemical characteristics of a drug molecule may make it unsuitable for oral delivery such as low aqueous solubility/stability that can by itself contribute to low oral bioavailability. To address these issues, nanoparticles have been widely investigated for oral delivery of small molecules and proteins/peptide drugs [13, 34-36] . The nano-sized particles provide a vehicle for controlled or sustained release of drugs and a larger contact surface area for adherence to the intestine that can improve absorption. Furthermore, nanoparticles can be produced from a wide variety of materials to modulate their physico-chemical characteristics and their surfaces can be modified in various ways to improve drug's oral bioavailability.
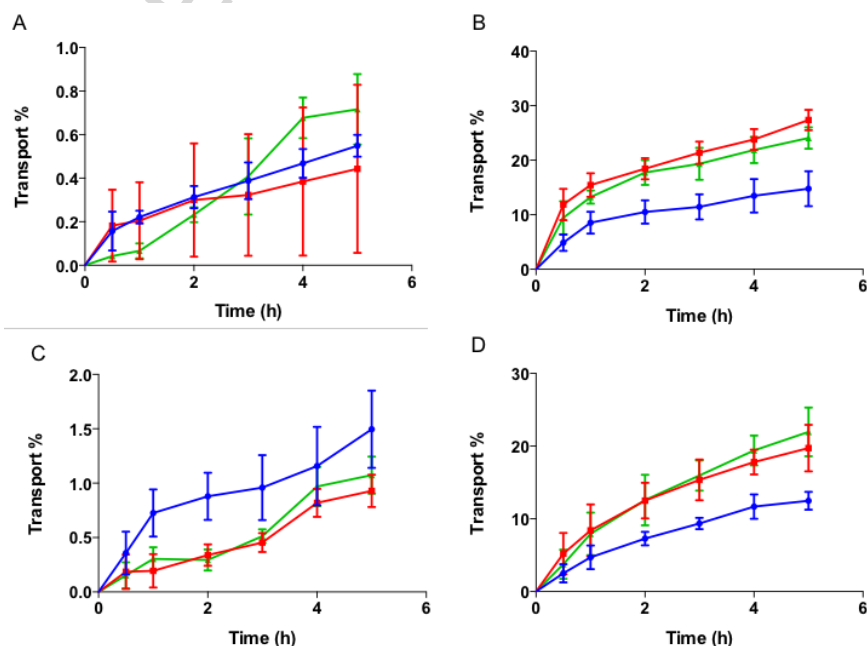

Figure 9: Transport of conjugated nanoparticles across intestinal cells. Transport of biotin-conjugated spheres, rods and discs across (A) Caco-2; (B) Caco-2/Raji-B; (C)

16

Caco-2/HT-29 and (D) Caco-2/HT-29/Raji-B cells. Conjugated spheres, rods and discs are represented as blue circles, red squares and green triangles respectively. As earlier observed, no significant transport of biotin-conjugated particles was seen across Caco-2 monolayer or Caco-2/HT-29 cells. Raji-B based co-cultures improved transport significantly and demonstrated shape dependent effect. Rods and discs were transported more than spheres across these co-cultures. Data represented as mean ± SD.

To prevent drug degradation in the stomach, drug loaded nanoparticles can either be enterically-coated or placed in an enterically-coated capsule for site specific and sustained delivery [37-39] . To increase the residence time of nanoparticles in the GIT, mucoadhesive nanoparticles have been used extensively. Nanoparticles prepared from polymers such as polylactic acid, poly(lactic-co-glycolic acid) (PLGA) or polyacrylic acid have mucoadhesive properties and have been used for oral delivery of docetaxel, tetanus toxoid, cyclosporine, insulin and silk peptide amongst many others [40-45] . Coating of nanoparticles with hydrophilic polymers such as PVA has also been shown to improve both mucoadhesion as well as oral uptake of the loaded drugs [46, 47] . Lipidic nanoparticles such as liposomes, solid lipid nanoparticles and mixed micelles have been used for oral delivery of both hydrophilic and poorly water soluble drugs like insulin, doxorubicin, simvastatin, efavirnez, and paclitaxel amongst others [11, 48-53] . Other polymeric materials such as chitosan and its derivative trimethyl chitosan based nanoparticles have also been widely used for oral delivery of drugs and genes due to their strong mucoadhesive property and ability to modulate intestinal permeability [54] . In addition, to improve drug uptake in the intestine, nanoparticles have been conjugated with peptidic or non-peptidic targeting ligands such as lectins, RGD peptide, transferrin, folic acid, biotin and mannose, to improve oral intestinal absorption of poorly permeable drugs [36, 55] .

However, despite such developments and innovations in the field of oral delivery using nanoparticles, not much deliberation has been made towards studying the influence of shape of nanoparticles on their uptake. Particles of different geometries can have dissimilar flow properties in the body and can interact with their biological targets as well as accumulate in the organs differently [56] . Previously, our laboratory has shown that compared to spherical particles, worm-like particles can be used to significantly inhibit phagocytosis by macrophages while actively targeted rod shaped particles can be used to achieve higher uptake in breast cancer cells as well as greater accumulation in brain and lungs [29, 57, 58] . This can be attributed to the larger surface area for contact and binding and lesser drag force that leads to higher internalization of rod shaped particles compared to spheres [59, 60] . A rational approach to nanoparticle design should therefore include particle size, shape and surface properties to maximize drug delivery, the information about which is not yet available in the field of oral drug delivery. Hence, in this study we investigated the influence of particle geometry in their uptake and transport across intestinal cells.

The study utilizing different sized nanoparticles demonstrated that smaller sized particles (50 and 200 nm) are taken up and transported across the intestinal cells more efficiently than larger sized particles. Similar results were reported by He *et al*. who

found that particles 300 nm in size or less are ideal for oral drug delivery since they are preferentially internalized by both enterocytes and M cells and demonstrate higher intestinal transport compared to larger sized particles [61] . Particle transport across Caco-2 monolayers or Caco-2/HT-29 cells was negligible. This is in accordance with the observation made by Hu X *et al*. who found that intact solid lipid nanoparticles when given orally were taken up by intestinal cells but did not translocate across cell monolayers [30] . PLGA nanoparticles were also found to show high uptake but low transcytosis when incubated with Caco-2 monolayer [62] . Including Raji-B cells in the cell culture, on the contrary, drastically improved transport of the particles. M cells have high endocytotic ability and have been reported to show high capability for transcytosis of drugs, macromolecules and nanoparticles [28, 36, 63] . Investigation of uptake of differently shaped unconjugated nanoparticles revealed that rods and discs were taken up two times more than spheres by Caco-2 cells while in Caco-2/HT-29 co-culture the difference in cellular uptake between rods and spheres was three fold. Biotin-conjugation increased uptake of rods by 3 fold and in spheres and discs by 2 fold in both Caco-2 cells and Caco-2/HT-29 co-cultures. In addition, the uptake of biotin-conjugated rods was 3 times higher than conjugated spheres while biotin-conjugated discs were taken up 2 times higher in both Caco-2 and Caco-2/HT-29 cells. The results clearly indicate that rods have higher cellular uptake by intestinal cells and attaching targeting ligand to particles further improves uptake. As explained earlier, the higher uptake of rods and discs over spheres is postulated to be due to larger contact surface area in rods and discs for interaction and adhesion with cell membranes that can kick-start uptake processes in cells [18, 64] . Rods were found to have about 2 times more surface area than spheres and about 1.5 times more surface area than discs. On the other hand, discs had $1.3 - 1.6$ times more surface area than spheres. Since the rods and discs were prepared from the same stock of 200 nm spheres, it enabled us to keep the volume of the particles constant while varying their surface areas. Along the same lines, a possible explanation for higher uptake of actively targeted rods compared to targeted discs and spheres is that rods due to their larger surface to volume ratio, present more sites for ligand conjugation, (Table 2) thereby increases the probability of locating and interacting with cellular receptors for uptake [29] .

The transport of nanoparticles across Caco-2 monolayer or Caco-2/HT-29 cells was negligible for all particles regardless of shape and ligand conjugation. As earlier observed, transport significantly increased in co-cultures containing Raji-B. No significant difference was found between triple co-culture or Caco-2/Raji-B co-culture, pointing towards the fact Raji-B cells are primarily responsible for improving transport of nanoparticles. This is also evident from the apparent permeability coefficient (Papp) values for transport (Tables 3 and 4). With regards to size, the Papp values consistently decrease with increase in particle size and co-cultures including Raji-B demonstrate higher transport compared to cultures without Raji-B (Table 3). 50 and 200 nm sized particles also exhibit significantly higher transport than 500 and 1000 nm sized particles. With regards to shape, the Papp values of rods are significantly higher than spheres (Table 4). The higher cellular uptake of rods as well as their smaller diameter may have contributed to their higher transport compared to spheres. Active targeting further significantly improved transport of rods compared to non-targeted rods. However, for all other particles, only a slight improvement in their transport was observed when actively

targeted particles were compared to non-targeted particles, which is in contrary to uptake results. A possible explanation is the presence of biotin receptors only on Caco-2 cells.

Table 3: Apparent permeability coefficient for transport of different sized particles across intestinal cell culture. # represents statistically significant difference between 50 nm spheres and 500/1000 nm spheres in the triple co-culture; No significant difference in the Papp values was found between 50 and 200 nm spheres. * represents statistically significant difference between 200 nm sized particles and 500/1000 nm sized particles. + represents significant difference between 500 nm spheres and 1000 nm spheres (p < 0.05). All statistical analysis was performed for Papp values obtained from triple co-culture only.

	Apparent Permeability coefficient (x 10^{-7} cm/sec)			
	Caco-2	**Caco-2/Raji-B**	**Caco-2/HT-29**	**Caco-2/HT-29/RajiB**
50 nm	2.8 ± 0.3	202.6 ± 42.01	4.1 ± 1.3	210.9 ± 8.6
200 nm	1.1 ± 0.4	167.4 ± 9	2.4 ± 1.3	188 ± 19.3
500 nm	0.2 ± 0.2	127.6 ± 6.3	2 ± 1.9	$142 \pm 9.7^{\#*}$
1000 nm	0.5 ± 0.04	60.5 ± 10.5	0.7 ± 0.2	$75.4 \pm 12.2^{\#*+}$

Table 4: Apparent permeability coefficient for transport of different shaped and surface modified particles across intestinal cell culture. # represents statistically significant difference between spheres and rods in the triple co-culture; No significant difference was found between spheres and discs or between rods and discs. * represents statistically significant difference between biotin-conjugated spheres with biotin-conjugated rods/discs. No difference was found between biotin-conjugated rods and biotin-conjugated discs. + represents significant difference between rods and biotin conjugated rods. No statistically significant difference was obtained between spheres and biotin-conjugated spheres or between discs and biotin-conjugated discs (p < 0.05). All statistical analysis was performed for Papp values obtained from triple co-culture only.

	Apparent Permeability coefficient (x 10^{-7} cm/sec)			
	Caco-2	**Caco-2/Raji-B**	**Caco-2/HT-29**	**Caco-2/HT-29/Raji-B**
Spheres	4.3 ± 1.1	101 ± 4.8	7.5 ± 1.9	92.4 ± 6.8
Biotin-Spheres	4.6 ± 0.3	117.8 ± 25.1	11.7 ± 2.8	113.7 ± 15.2
Rods	4.1 ± 1	163.5 ± 9.1	4.8 ± 1.4	$134 \pm 10.5^{\#}$
Biotin-Rods	5.1 ± 0.3	204.8 ± 6.7	8.6 ± 1.6	$170.4 \pm 9.9^{*+}$

Discs	10.4 ± 9.1	171.3 ± 5.8	7.2 ± 1.6	163.2 ± 38.4
Biotin-Discs	7.5 ± 1.7	188.5 ± 11.9	9.8 ± 1.2	$199.7 \pm 18.7^{*}$

Taken together, the findings from this work clearly depict that particle geometry has a substantial impact on oral uptake and transport of nanoparticles. Moreover, particle geometry can significantly impact solubilization of poorly water-soluble drugs, where increase in particle surface area can notably improve solubilization of such drugs. In light of higher surface area of rods compared to spheres, pure drug nanorods can essentially improve drug dissolution properties, hence oral drug delivery compared to spheres. Therefore, due consideration should be given to selecting the appropriate particle size and shape to maximize the effectiveness of nanoparticles developed for oral drug delivery.

Conclusion

Nanoparticles have been extensively used for delivery of drugs with inherent poor oral bioavailability. However, apart from classical spherical nanoparticles, no other shapes have been explored for oral drug delivery. In this study, we present, for the first time, the role of nanoparticle geometry and surface chemistry in their uptake and transport across intestinal cells. Using polystyrene particles of different sizes and shapes, we demonstrated that rod-shaped particles have higher cellular uptake and transport across intestinal cells compared to spherical particles. Actively targeted rods also accumulated to a greater extent in the cells compared to targeted spheres or discs. The study lays the foundation for rational design of nanoparticles for oral drug delivery. We believe that rod-shaped nanoparticles can potentially improve the efficacy of nanoparticles in oral drug delivery. However, *in vivo* studies are required to validate the *in vitro* results. Additional studies using biodegradable nanoparticles and scale-up studies addressing bulk manufacturing issues such flowability of elongated particles are also needed before actual clinical application of rod shaped nanoparticles in oral drug delivery. Studies using different shaped nanoparticles but with similar surface area to volume ratio constitutes an additional interesting premise for investigation as well and should also be performed in future.

References

[1]. Goldberg M, Gomez-Orellana I. , Challenges for the oral delivery of macromolecules, Nat Rev Drug Discov. (2003) 2(4) 289-95. DOI:10.1038/nrd1067 [doi].

[2]. Banerjee A, Onyuksel H. , Peptide delivery using phospholipid micelles, Wiley Interdiscip Rev Nanomed Nanobiotechnol. (2012) 4(5) 562-74. DOI:10.1002/wnan.1185; 10.1002/wnan.1185.

[3]. Fu AZ, Qiu Y, Radican L. , Impact of fear of insulin or fear of injection on treatment outcomes of patients with diabetes, Curr Med Res Opin. (2009) 25(6) 1413-20. DOI:10.1185/03007990902905724 [doi].

[4]. Gupta H, Bhandari D, Sharma A. , Recent trends in oral drug delivery: a review, Recent Pat Drug Deliv Formul. (2009) 3(2) 162-73.

[5]. Sastry SV, Nyshadham JR, Fix JA. , Recent technological advances in oral drug delivery – a review, Pharm Sci Technol Today. (2000) 3(4) 138-45. DOI:http://dx.doi.org/10.1016/S1461-5347(00)00247-9.

[6]. Mrsny RJ. , Oral drug delivery research in Europe, J Controlled Release. (2012) 161(2) 247-53. DOI:http://dx.doi.org/10.1016/j.jconrel.2012.01.017.

[7]. Banerjee A, Lee J, Mitragotri S. , Intestinal Mucoadhesive Devices for Oral Delivery of Insulin, Bioeng Transl Med. (2016) In press. DOI:http://dx.doi.org/10.1002/btm2.10015

[8]. Iannuccelli V, Montanari M, Bertelli D, Pellati F, Coppi G. , Microparticulate polyelectrolyte complexes for gentamicin transport across intestinal epithelia, Drug Deliv. (2011) 18(1) 26-37. DOI:10.3109/10717544.2010.509362 [doi].

[9]. Huang X, Xiao Y, Lang M. , Micelles/sodium-alginate composite gel beads: A new matrix for oral drug delivery of indomethacin, Carbohydr Polym. (2012) 87(1) 790-8. DOI:http://dx.doi.org/10.1016/j.carbpol.2011.08.067.

[10]. Momin M, Pundarikakshudu K, Nagori SA. , Design and development of mixed film of pectin: ethyl cellulose for colon specific drug delivery of sennosides and triphala, Indian J Pharm Sci. (2008) 70(3) 338-43. DOI:10.4103/0250-474X.42998 [doi].

[11]. Kalepu S, Manthina M, Padavala V. , Oral lipid-based drug delivery systems – an overview, Acta Pharmaceutica Sinica B. (2013) 3(6) 361-72. DOI:http://dx.doi.org/10.1016/j.apsb.2013.10.001.

[12]. Mullertz A, Ogbonna A, Ren S, Rades T. , New perspectives on lipid and surfactant based drug delivery systems for oral delivery of poorly soluble drugs, J Pharm Pharmacol. (2010) 62(11) 1622-36. DOI:10.1111/j.2042-7158.2010.01107.x [doi].

[13]. Ensign LM, Cone R, Hanes J. , Oral drug delivery with polymeric nanoparticles: The gastrointestinal mucus barriers, Adv Drug Deliv Rev. (2012) 64(6) 557-70. DOI:http://dx.doi.org/10.1016/j.addr.2011.12.009.

[14]. Allémann E, Leroux J, Gurny R. , Polymeric nano- and microparticles for the oral delivery of peptides and peptidomimetics, Adv Drug Deliv Rev. (1998) 34(2–3) 171-89. DOI:http://dx.doi.org/10.1016/S0169-409X(98)00039-8.

[15]. Chen M, Sonaje K, Chen K, Sung H. , A review of the prospects for polymeric nanoparticle platforms in oral insulin delivery, Biomaterials. (2011) 32(36) 9826-38. DOI:http://dx.doi.org/10.1016/j.biomaterials.2011.08.087.

[16]. Kumar S, Anselmo AC, Banerjee A, Zakrewsky M, Mitragotri S. , Shape and size-dependent immune response to antigen-carrying nanoparticles, J Controlled Release. (2015) 220, Part A 141-8. DOI:http://dx.doi.org/10.1016/j.jconrel.2015.09.069.

[17]. Champion JA, Katare YK, Mitragotri S. , Particle shape: A new design parameter for micro-and nanoscale drug delivery carriers, J Controlled Release. (2007) 121(1–2) 3-9. DOI:http://dx.doi.org/10.1016/j.jconrel.2007.03.022.

[18]. Muro S, Garnacho C, Champion JA, Leferovich J, Gajewski C, Schuchman EH, et al. , Control of endothelial targeting and intracellular delivery of therapeutic enzymes by modulating the size and shape of ICAM-1-targeted carriers, Mol Ther. (2008) 16(8) 1450-8. DOI:10.1038/mt.2008.127 [doi].

[19]. Doshi N, Mitragotri S. , Macrophages recognize size and shape of their targets, PLoS One. (2010) 5(4) e10051. DOI:10.1371/journal.pone.0010051 [doi].

[20]. Champion JA, Mitragotri S. , Role of target geometry in phagocytosis, Proc Natl Acad Sci U S A. (2006) 103(13) 4930-4. DOI:0600997103 [pii].

[21]. Chatterjee NS, Kumar CK, Ortiz A, Rubin SA, Said HM. , Molecular mechanism of the intestinal biotin transport process, Am J Physiol. (1999) 277(4 Pt 1) C605-13.

[22]. Zhang X, Qi J, Lu Y, Hu X, He W, Wu W. , Enhanced hypoglycemic effect of biotin-modified liposomes loading insulin: effect of formulation variables, intracellular trafficking, and cytotoxicity, Nanoscale Res Lett. (2014) 9(1) 185,276X-9-185. eCollection 2014. DOI:10.1186/1556-276X-9-185 [doi].

[23]. Ma TY, Dyer DL, Said HM. , Human intestinal cell line Caco-2: a useful model for studying cellular and molecular regulation of biotin uptake, Biochim Biophys Acta. (1994) 1189(1) 81-8. DOI:0005-2736(94)90283-6 [pii].

[24]. Chae SY, Jin CH, Shin HJ, Youn YS, Lee S, Lee KC. , Preparation, characterization, and application of biotinylated and biotin-PEGylated glucagon-like peptide-1 analogues for enhanced oral delivery, Bioconjug Chem. (2008) 19(1) 334-41. DOI:10.1021/bc700292v [doi].

[25]. Sun H, Chow EC, Liu S, Du Y, Pang KS. , The Caco-2 cell monolayer: usefulness and limitations, Expert Opin Drug Metab Toxicol. (2008) 4(4) 395-411. DOI:10.1517/17425255.4.4.395 [doi].

[26]. Araújo F, Sarmento B. , Towards the characterization of an in vitro triple co-culture intestine cell model for permeability studies, Int J Pharm. (2013) 458(1) 128-34. DOI:http://dx.doi.org/10.1016/j.ijpharm.2013.10.003.

[27]. Antunes F, Andrade F, Araújo F, Ferreira D, Sarmento B. , Establishment of a triple co-culture in vitro cell models to study intestinal absorption of peptide drugs, European J Pharmaceutics and Biopharmaceutics. (2013) 83(3) 427-35. DOI:http://dx.doi.org/10.1016/j.ejpb.2012.10.003.

[28]. Schimpel C, Teubl B, Absenger M, Meindl C, Frohlich E, Leitinger G, et al. , Development of an advanced intestinal in vitro triple culture permeability model to study transport of nanoparticles, Mol Pharm. (2014) 11(3) 808-18. DOI:10.1021/mp400507g [doi].

[29]. Barua S, Yoo JW, Kolhar P, Wakankar A, Gokarn YR, Mitragotri S. , Particle shape enhances specificity of antibody-displaying nanoparticles, Proc Natl Acad Sci U S A. (2013) 110(9) 3270-5. DOI:10.1073/pnas.1216893110 [doi].

[30]. Hu X, Fan W, Yu Z, Lu Y, Qi J, Zhang J, et al. , Evidence does not support absorption of intact solid lipid nanoparticles via oral delivery, Nanoscale. (2016) DOI:10.1039/c5nr07474f [doi].

[31]. Kadiyala I, Loo Y, Roy K, Rice J, Leong KW. , Transport of chitosan–DNA nanoparticles in human intestinal M-cell model versus normal intestinal enterocytes, European J Pharmaceutical Sciences. (2010) 39(1–3) 103-9. DOI:http://dx.doi.org/10.1016/j.ejps.2009.11.002.

[32]. Loo Y, Grigsby CL, Yamanaka YJ, Chellappan MK, Jiang X, Mao H, et al. , Comparative study of nanoparticle-mediated transfection in different GI epithelium co-culture models, J Controlled Release. (2012) 160(1) 48-56. DOI:http://dx.doi.org/10.1016/j.jconrel.2012.01.041.

[33]. des Rieux A, Fievez V, Théate I, Mast J, Préat V, Schneider Y. , An improved in vitro model of human intestinal follicle-associated epithelium to study nanoparticle transport by M cells, European J Pharmaceutical Sciences. (2007) 30(5) 380-91. DOI:http://dx.doi.org/10.1016/j.ejps.2006.12.006.

[34]. Galindo-Rodriguez SA, Allemann E, Fessi H, Doelker E. , Polymeric nanoparticles for oral delivery of drugs and vaccines: a critical evaluation of in vivo studies, Crit Rev Ther Drug Carrier Syst. (2005) 22(5) 419-64. DOI:0f80ebac03395679,2df4fcbf590f75da [pii].

[35]. des Rieux A, Fievez V, Garinot M, Schneider Y, Préat V. , Nanoparticles as potential oral delivery systems of proteins and vaccines: A mechanistic approach, J Controlled Release. (2006) 116(1) 1-27. DOI:http://dx.doi.org/10.1016/j.jconrel.2006.08.013.

[36]. Yun Y, Cho YW, Park K. , Nanoparticles for oral delivery: Targeted nanoparticles with peptidic ligands for oral protein delivery, Adv Drug Deliv Rev. (2013) 65(6) 822-32. DOI:http://dx.doi.org/10.1016/j.addr.2012.10.007.

[37]. Tummala S, Satish Kumar MN, Prakash A. , Formulation and characterization of 5-Fluorouracil enteric coated nanoparticles for sustained and localized release in treating colorectal

cancer, Saudi Pharmaceutical J. (2015) 23(3) 308-14. DOI:http://dx.doi.org/10.1016/j.jsps.2014.11.010.

[38]. Wang X, Zhang Q. , pH-sensitive polymeric nanoparticles to improve oral bioavailability of peptide/protein drugs and poorly water-soluble drugs, European J Pharmaceutics and Biopharmaceutics. (2012) 82(2) 219-29. DOI:http://dx.doi.org/10.1016/j.ejpb.2012.07.014.

[39]. Sonaje K, Chen Y, Chen H, Wey S, Juang J, Nguyen H, et al. , Enteric-coated capsules filled with freeze-dried chitosan/poly(γ-glutamic acid) nanoparticles for oral insulin delivery, Biomaterials. (2010) 31(12) 3384-94. DOI:http://dx.doi.org/10.1016/j.biomaterials.2010.01.042.

[40]. Feng S, Mei L, Anitha P, Gan CW, Zhou W. , Poly(lactide)–vitamin E derivative/montmorillonite nanoparticle formulations for the oral delivery of Docetaxel, Biomaterials. (2009) 30(19) 3297-306. DOI:http://dx.doi.org/10.1016/j.biomaterials.2009.02.045.

[41]. Tobío M, Sánchez A, Vila A, Soriano I, Evora C, Vila-Jato JL, et al. , The role of PEG on the stability in digestive fluids and in vivo fate of PEG-PLA nanoparticles following oral administration, Colloids and Surfaces B: Biointerfaces. (2000) 18(3–4) 315-23. DOI:http://dx.doi.org/10.1016/S0927-7765(99)00157-5.

[42]. Italia JL, Bhatt DK, Bhardwaj V, Tikoo K, Kumar MNVR. , PLGA nanoparticles for oral delivery of cyclosporine: Nephrotoxicity and pharmacokinetic studies in comparison to Sandimmune Neoral®, J Controlled Release. (2007) 119(2) 197-206. DOI:http://dx.doi.org/10.1016/j.jconrel.2007.02.004.

[43]. Cui FD, Tao AJ, Cun DM, Zhang LQ, Shi K. , Preparation of insulin loaded PLGA-Hp55 nanoparticles for oral delivery, J Pharm Sci. (2007) 96(2) 421-7. DOI:10.1002/jps.20750 [doi].

[44]. Hu Y, Jiang X, Ding Y, Ge H, Yuan Y, Yang C. , Synthesis and characterization of chitosan–poly(acrylic acid) nanoparticles, Biomaterials. (2002) 23(15) 3193-201. DOI:http://dx.doi.org/10.1016/S0142-9612(02)00071-6.

[45]. Foss AC, Goto T, Morishita M, Peppas NA. , Development of acrylic-based copolymers for oral insulin delivery, European J Pharmaceutics and Biopharmaceutics. (2004) 57(2) 163-9. DOI:http://dx.doi.org/10.1016/S0939-6411(03)00145-0.

[46]. Yin Win K, Feng S. , Effects of particle size and surface coating on cellular uptake of polymeric nanoparticles for oral delivery of anticancer drugs, Biomaterials. (2005) 26(15) 2713-22. DOI:http://dx.doi.org/10.1016/j.biomaterials.2004.07.050.

[47]. Yang M, Lai SK, Yu T, Wang YY, Happe C, Zhong W, et al. , Nanoparticle penetration of human cervicovaginal mucus: the effect of polyvinyl alcohol, J Control Release. (2014) 192 202-8. DOI:10.1016/j.jconrel.2014.07.045 [doi].
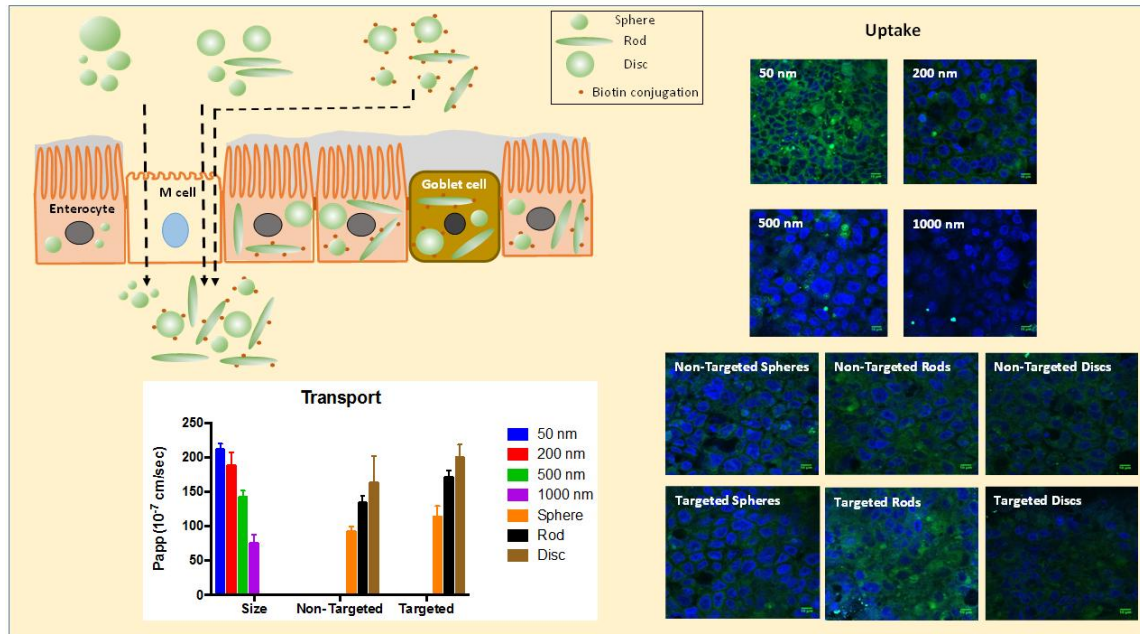
[48]. Padhye SG, Nagarsenker MS. , Simvastatin Solid Lipid Nanoparticles for Oral Delivery: Formulation Development and In vivo Evaluation, Indian J Pharm Sci. (2013) 75(5) 591-8.

[49]. Zhang N, Ping Q, Huang G, Xu W, Cheng Y, Han X. , Lectin-modified solid lipid nanoparticles as carriers for oral administration of insulin, Int J Pharm. (2006) 327(1–2) 153-9. DOI:http://dx.doi.org/10.1016/j.ijpharm.2006.07.026.

[50]. Gaur PK, Mishra S, Bajpai M, Mishra A. , Enhanced oral bioavailability of efavirenz by solid lipid nanoparticles: in vitro drug release and pharmacokinetics studies, Biomed Res Int. (2014) 2014 363404. DOI:10.1155/2014/363404 [doi].

[51]. Jain S, Patil SR, Swarnakar NK, Agrawal AK. , Oral delivery of doxorubicin using novel polyelectrolyte-stabilized liposomes (layersomes), Mol Pharm. (2012) 9(9) 2626-35. DOI:10.1021/mp300202c [doi].

[52]. Jain S, Kumar D, Swarnakar NK, Thanki K. , Polyelectrolyte stabilized multilayered liposomes for oral delivery of paclitaxel, Biomaterials. (2012) 33(28) 6758-68. DOI:http://dx.doi.org/10.1016/j.biomaterials.2012.05.026.

[53]. Gaucher G, Satturwar P, Jones M, Furtos A, Leroux J. , Polymeric micelles for oral drug delivery, European J Pharmaceutics and Biopharmaceutics. (2010) 76(2) 147-58. DOI:http://dx.doi.org/10.1016/j.ejpb.2010.06.007.

[54]. Bowman K, Leong KW. , Chitosan nanoparticles for oral drug and gene delivery, Int J Nanomedicine. (2006) 1(2) 117-28.

[55]. des Rieux A, Pourcelle V, Cani PD, Marchand-Brynaert J, Préat V. , Targeted nanoparticles with novel non-peptidic ligands for oral delivery, Adv Drug Deliv Rev. (2013) 65(6) 833-44. DOI:http://dx.doi.org/10.1016/j.addr.2013.01.002.

[56]. Blanco E, Shen H, Ferrari M. , Principles of nanoparticle design for overcoming biological barriers to drug delivery, Nat Biotechnol. (2015) 33(9) 941-51. DOI:10.1038/nbt.3330 [doi].

[57]. Champion JA, Mitragotri S. , Shape induced inhibition of phagocytosis of polymer particles, Pharm Res. (2009) 26(1) 244-9. DOI:10.1007/s11095-008-9626-z [doi].

[58]. Kolhar P, Anselmo AC, Gupta V, Pant K, Prabhakarpandian B, Ruoslahti E, et al. , Using shape effects to target antibody-coated nanoparticles to lung and brain endothelium, Proc Natl Acad Sci U S A. (2013) 110(26) 10753-8. DOI:10.1073/pnas.1308345110 [doi].

[59]. Sharma G, Valenta DT, Altman Y, Harvey S, Xie H, Mitragotri S, et al. , Polymer particle shape independently influences binding and internalization by macrophages, J Controlled Release. (2010) 147(3) 408-12. DOI:http://dx.doi.org/10.1016/j.jconrel.2010.07.116.

[60]. Tan J, Shah S, Thomas A, Ou-Yang HD, Liu Y. , The influence of size, shape and vessel geometry on nanoparticle distribution, Microfluid Nanofluidics. (2013) 14(1-2) 77-87. DOI:10.1007/s10404-012-1024-5 [doi].

[61]. He C, Yin L, Tang C, Yin C. , Size-dependent absorption mechanism of polymeric nanoparticles for oral delivery of protein drugs, Biomaterials. (2012) 33(33) 8569-78. DOI:http://dx.doi.org/10.1016/j.biomaterials.2012.07.063.

[62]. He B, Lin P, Jia Z, Du W, Qu W, Yuan L, et al. , The transport mechanisms of polymer nanoparticles in Caco-2 epithelial cells, Biomaterials. (2013) 34(25) 6082-98. DOI:http://dx.doi.org/10.1016/j.biomaterials.2013.04.053.

[63]. Kucharzik T, Lugering N, Rautenberg K, Lugering A, Schmidt MA, Stoll R, et al. , Role of M cells in intestinal barrier function, Ann N Y Acad Sci. (2000) 915 171-83.

[64]. Agarwal R, Singh V, Jurney P, Shi L, Sreenivasan SV, Roy K. , Mammalian cells preferentially internalize hydrogel nanodiscs over nanorods and use shape-specific uptake mechanisms, Proc Natl Acad Sci U S A. (2013) 110(43) 17247-52. DOI:10.1073/pnas.1305000110 [doi].

Graphical abstract